

Multi-stimuli Responsive Supramolecular Diblock Copolymers

L. Sambe, K. Belal, F. Stoffelbach,* J. Lyskawa, F. Delattre, M. Bria, F. X. Sauvage, M. Sliwa, V. Humblot, B. Charleux, G. Cooke* and P. Woisel*

Table of contents

A) Materials	p 2
B) Instruments and measurements	p 2
C) Synthesis of materials	p 3
I. Synthesis and characterization of the reversible chain transfer agent 2	p 3
II. Synthesis of polymers 3, 6a,b and 7a,b	p 8
III. Characterization of polymers 3, 6a,b and 7a,b	p 9
a) Characterization of CBPQT ⁴⁺ end-functionalized poly(<i>n</i> -butyl acrylate) 3	p 10
b) Characterization of naphthalene end-functionalized Poly(<i>N</i> -isopropyl-acrylamide) 6a	p 11
c) Characterization of naphthalene end-functionalized Poly(<i>N,N</i> -dimethyl-acrylamide) 6b	p 12
d) Characterization of TTF end-functionalized Poly(<i>N</i> -isopropylacrylamide) 7a	p 13
e) Characterization of TTF end-functionalized Poly(<i>N,N</i> -dimethylacrylamide) 7b	p 14
D) Binding studies	
a) Binding studies between 3 and 4	p 15
b) Binding studies between 3 and 5	p 17
c) Binding studies between 3 and 6a	p 19
d) Binding studies between 3 and 6b	p 21
e) Binding studies between 3 and 7a	p 23
f) Binding studies between 3 and 7b	p 25
g) Binding studies: summary of the ¹ H NMR and voltammetric data	p 27
h) Control of binding events upon heating: UV-vis data	p 28
i) Control of binding events upon the addition of TTF: UV-vis and ¹ H NMR data	p 29
E) Nanostructuration of 3.7b in water and in thin films: UV-vis and AFM data	p 29
F) References	p 32

A) Materials

All reagents were purchased from Sigma-Aldrich and were used as received unless otherwise mentioned. *n*-Butyl acrylate (>99%, Acros Organics) and *N,N*-dimethylacrylamide were purified by distillation under reduced pressure at room temperature before use.

All polymerizations were conducted under an argon atmosphere.

B) Instruments and Measurements

UV-vis measurements were carried out on a Varian Cary 50 Scan UV/vis spectrophotometer equipped with a single cell Peltier temperature controller.

The electrochemical experiments were performed using an Autolab PGSTAT 30 workstation. A three electrode configuration was used with a platinum disc (2 mm diameter) as working electrode, an Ag/AgCl reference electrode, and a platinum wire as the counter electrode. The solution was purged with nitrogen prior to recording the electrochemical data, and all measurements were recorded at 298K under a nitrogen atmosphere.

The spectroelectrochemistry studies were performed on a Varian Cary 50 Scan UV/vis spectrophotometer and by using a thin layer (optical path cell: 0.5 mm) quartz glass spectroelectrochemical cell (Biologic Science Instruments).

¹H NMR and ¹³C spectra were recorded at 298K, with a Bruker Avance 300 spectrometer.

Fourier transform infrared (FTIR) spectra were recorded using a PerkinElmer Spectrum One FTIR spectrometer with a resolution of 4 cm⁻¹.

The number-average molar mass (M_n), the weight-average molar mass (M_w) and the polydispersity index ($D = M_w/M_n$) were determined by size exclusion chromatography (SEC) in DMF (+ LiBr, 1 g/L) at 60°C and at a flow rate of 0.8 mL min⁻¹ for PNIPAM and PDMAC polymers. The steric exclusion was carried out on two PSS GRAM 1000 Å columns (8 × 300 mm; separation limits: 1 to 1000 kg mol⁻¹) and one PSS GRAM 30 Å (8 × 300 mm; separation limits: 0.1 to 10 kg mol⁻¹) coupled with a differential refractive index (RI) detector. Average molar masses were derived from a calibration curve based on poly(methyl methacrylate) standards from Polymer Standards Service.

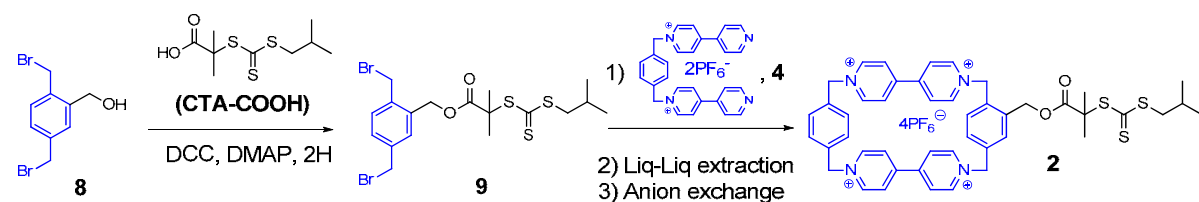
Association constants (K_a) for **3.4**, **3.5**, **3.6_{a-b}**, and **3.7_{a-b}** complexes were estimated using the spectrophotometric dilution method.¹ Briefly, assuming that complexes formed between **3** and guests molecules **4**, **5**, **6_{a-b}**, and **7_{a-b}** have 1:1 stoichiometry and that complexes with other stoichiometry do not exist, the plot of C/A against 1/A^{1/2} for a series of solutions of different

concentrations C should follow the relationship (1) and, thus, should afford a straight line with a slope equal to $(1/K_a \epsilon l)^{1/2}$ and the intercept y_0 equal to $1/\epsilon l$. The free energy of complexation ($-\Delta G^\circ$) was calculated using the relationship $\Delta G^\circ = -RT \ln K_a$, where R is the gas constant and T is the absolute temperature.

$$C/A = (1/K_a \epsilon l)^{1/2} \cdot 1/A^{1/2} + 1/\epsilon l \quad (1)$$

C) Synthesis of materials

I. Synthesis and characterization of the reversible chain transfer agent **2**



Compound **8**,² 1,1'-[1,4-phenylenebis(methylene)]bis-4,4'-bipyridinium Bis (hexafluorophosphate),³ **4**, and 2-(1-isobutyl)sulfanylthiocarbonylsulfanyl-2-methylpropionic acid **CTA-COOH**⁵ were synthesized as previously described.

Synthesis of **9**

Alcohol **8** (2 g, 6.8 mmol), 2-(1-isobutyl)sulfanylthiocarbonylsulfanyl-2-methylpropionic acid (1.7 g, 6.8 mmol), 1,3-dicyclohexylcarbodiimide (DCC) (1.4 g, 6.8 mmol) and 4-dimethylaminopyridine (DMAP) (catalytic amount) were dissolved in dry DCM (100 mL). The mixture was stirred 2 h under a nitrogen atmosphere at room temperature. The resulting suspension was filtered and the filtrate was concentrated under reduced pressure. The crude product was then subjected to column chromatography (SiO₂: petroleum ether / DCM, 1:1) to afford **9** (2.5 g, 70 %) as a yellow oil.

¹H NMR (300 MHz, CDCl₃), δ (ppm from TMS) : 7.39 (br, 1H), 7.33 (d, *J*= 1.2 Hz, 2H), 5.25 (s, 2H), 4.55 (s, 2H), 4.46 (s, 2H), 3.16 (d, *J*= 6.8 Hz, 2H), 2.01-1.87 (m, *J*= 6.7 Hz, 1H), 1.72 (s, 6H), 1.0 (d, *J*= 6.5 Hz, 6H).

¹³C NMR (75 MHz, CDCl₃), δ (ppm): 221.5, 172.8, 138.9, 136.9, 134.7, 131.2, 131.0, 129.7, 64.8, 55.9, 45.4, 32.6, 30.1, 30.0, 25.5, 22.2.

IR (cm⁻¹, KBr): 3041, 2965, 2929, 1725, 1639, 1459, 1363, 1243, 1219, 1121, 1056, 987, 828, 808.

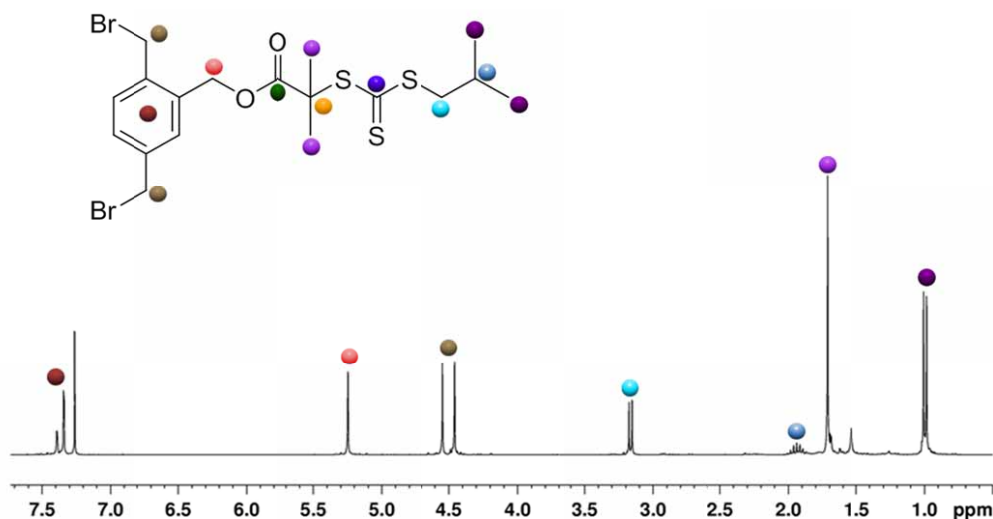


Figure S1. ¹H NMR spectrum of **9**. Recorded in CDCl₃ at 298K

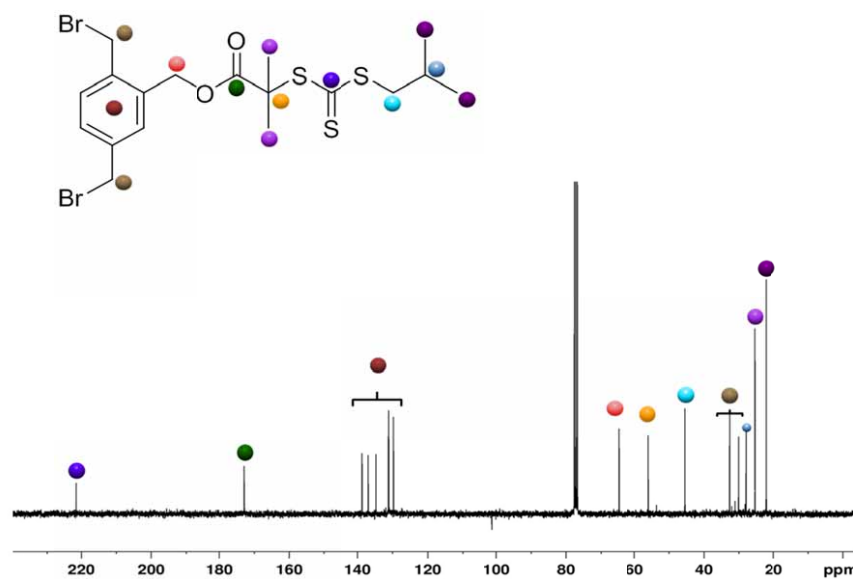


Figure S2. ¹³C NMR spectrum of **9**. Recorded in CDCl₃ at 298K

Synthesis and characterisation of the CTA agent **2**

To a solution containing the bipyridium salt (0.78 g, 1.1 mmol) and template **4** (1.1 g, 3.3 mmol) in dry DMF (300 mL) was added **9** (0.58 g, 1.1 mmol). The resulting solution was then stirred under a nitrogen atmosphere at room temperature for 10 days. The crude product was precipitated in Et₂O and the residue was subjected to a liquid-liquid extraction (DCM / H₂O). The aqueous layer was concentrated and the residue was purified by column chromatography (SiO₂: MeOH / NH₄Cl (2 M) / MeNO₂, 4:2:1.5). The fractions containing the product were combined and concentrated under reduced pressure. The residue was dissolved in hot water

and a saturated aqueous solution of NH_4PF_6 was added. The precipitate was collected by filtration, washed with water and Et_2O , and finally dried under vacuum to afford the RAFT agent **2** (0.36 g, 24 %) as a yellow solid.

^1H NMR (300 MHz, CD_3CN), δ (ppm from TMS) : 8.83-8.69 (brs, 8H), 8.21-8.08 (brs, 8H), 7.62-7.26 (brs, 7H), 5.86-5.76 (brs, 8H), 5.22 (s, 2H), 3.15 (d, $J= 6.8$ Hz, 2H), 1.85 (m, 1H), 1.69 (s, 6H), 0.96 (d, $J= 6.7$ Hz, 6H).

^{13}C NMR (75 MHz, CD_3CN), δ (ppm): 223.77, 173.07, 150.92, 150.56, 146.63, 146.41, 146.05, 137.10, 137.04, 136.90, 135.48, 133.07, 133.01, 131.35, 131.23, 131.09, 128.61, 128.36, 128.28, 65.72, 65.63, 65.42, 65.26, 62.17, 56.94, 45.93, 28.75, 25.51, 22.05.

IR (cm^{-1} , KBr): 3661, 3589, 3136, 3070, 2963, 1728, 1637, 1561, 1505, 1448, 1258, 1155, 1124, 1059, 1040, 814, 782.

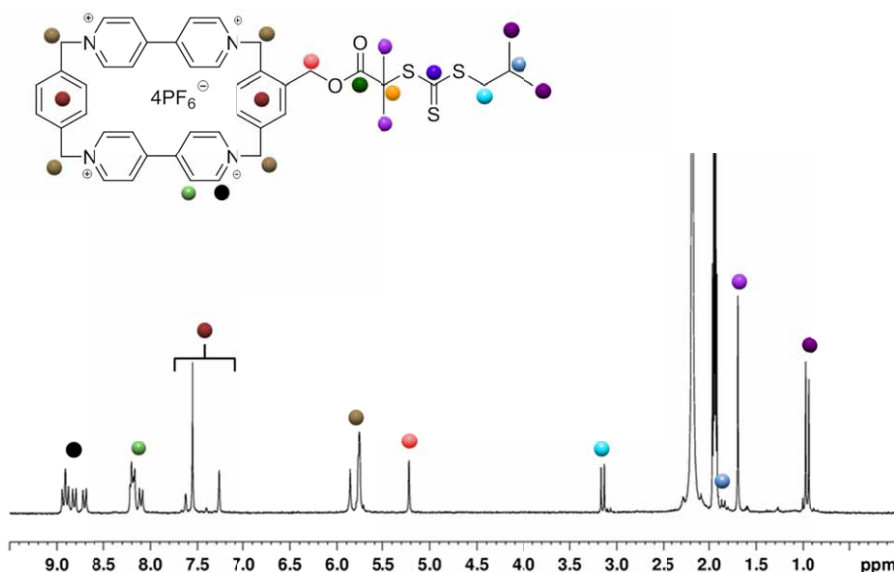


Figure S3. ^1H NMR spectrum of CTA agent **2** recorded in CD_3CN at 298K

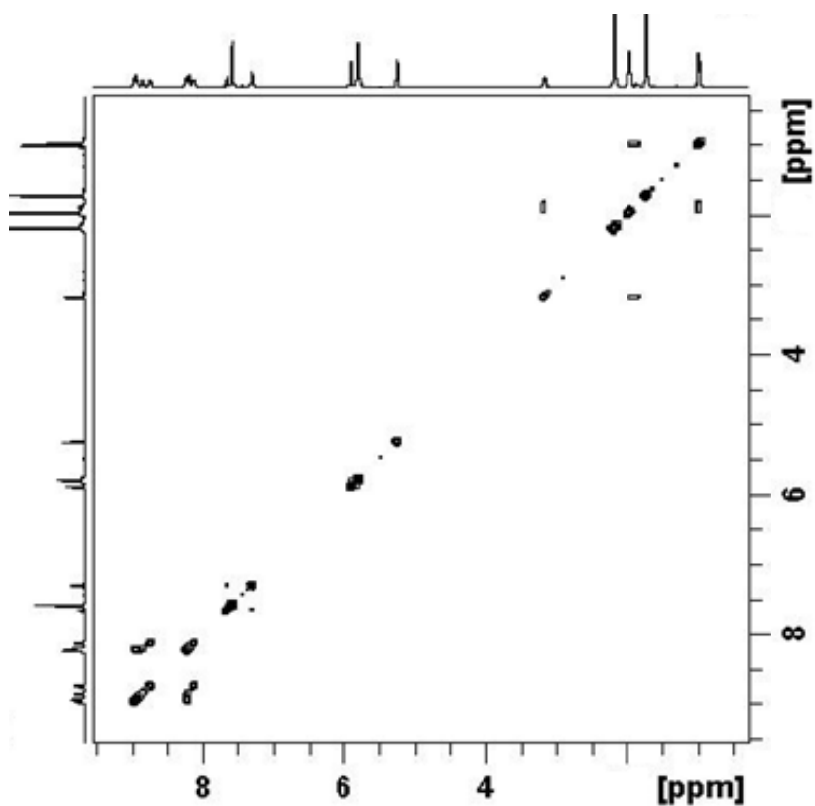


Figure S4. COSY spectrum of **2** recorded in CD_3CN at 298K

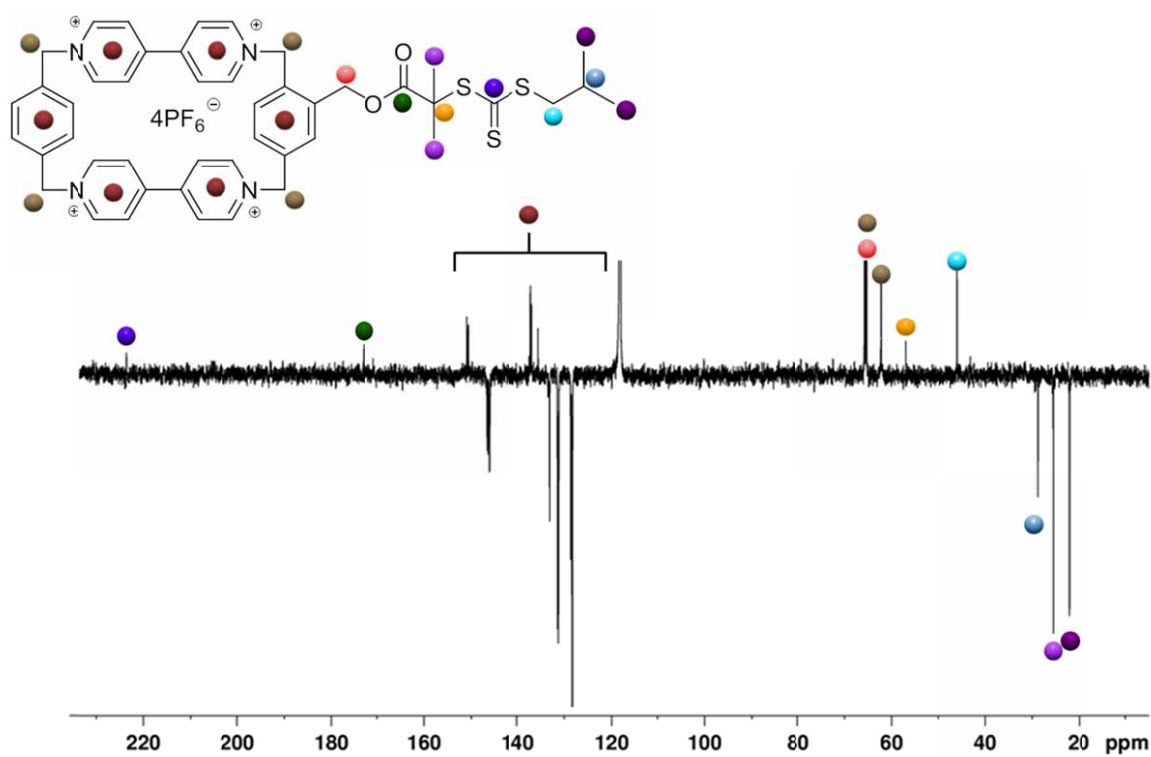


Figure S5. J MOD ^{13}C NMR spectrum of CTA agent **2** recorded in CD_3CN at 298K

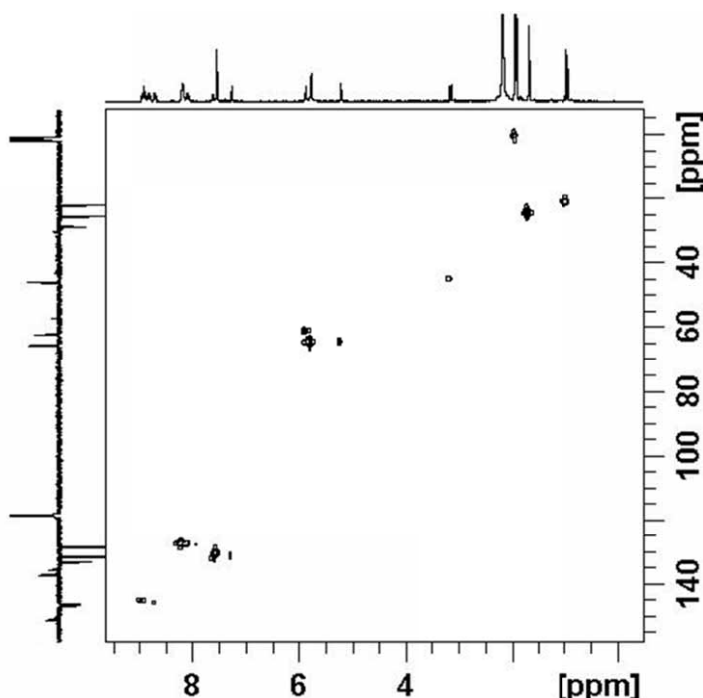


Figure S6. HMQC spectrum of **2** recorded in CD_3CN at 298K

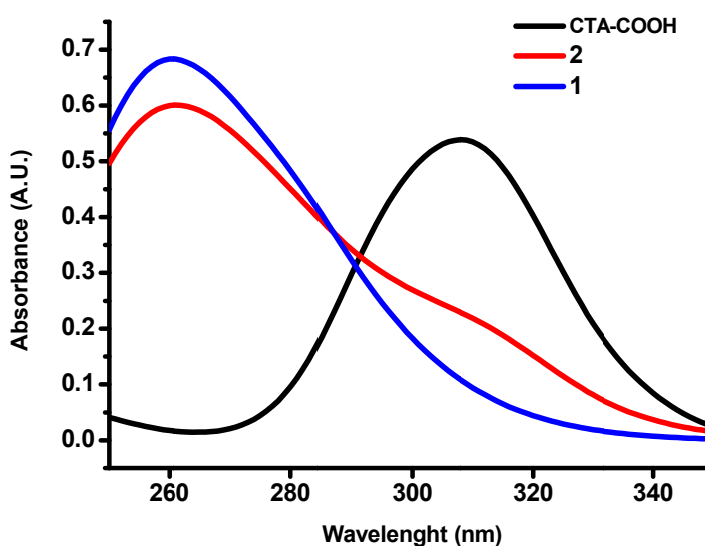
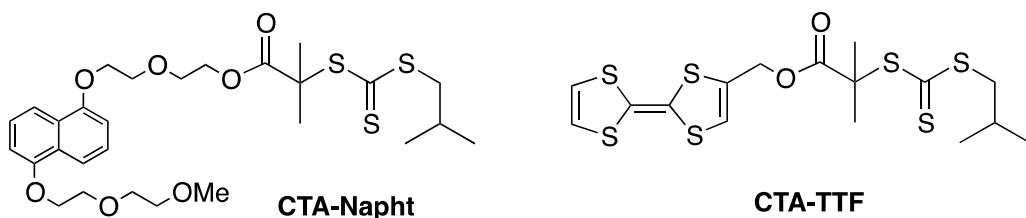


Figure S7. UV-vis spectra of **1** (blue curve), **2** (red curve) and **CTA-COOH** (black curve) recorded in CH_3CN (0.5 mM) at 298K.

UV-vis spectrum of **2** (Figure S7) clearly displays the characteristic absorption bands of the cyclophane moiety (260 nm) and the trithiocarbonate function (of around 310 nm).

II. Synthesis of polymers **3**, **6a,b** and **7a,b**

Polymers **6a**⁶ and **7a**⁷ were synthesized according to previously described procedures using CTA-Napht and CTA-TTF as RAFT agents, respectively.



Synthesis of CBPQT⁴⁺ end-functionalized poly(*n*-butyl acrylate) **3**

0.233 g (0.17 mmol) of CTA 2 was dissolved in 8mL of DMF in a 25 mL round-bottom flask. 5.6 mg (0.034 mmol) of AIBN were added and the resulting mixture was purged with nitrogen for 20 min in a cold water bath. After being deoxygenated by bubbling with nitrogen for 20 min, the *n*-butyl acrylate (3.5 g, 27.3 mmol) was injected through the septum into the reaction mixture. The sealed round-bottom flask was immersed in a thermostated oil bath at 343 K, and the polymerization lasted for 4.5 h. Samples were periodically withdrawn i) to measure the conversion by ¹H NMR spectroscopy in CDCl₃ by the relative integration of the methylenic proton peak (COO-CH₂) at 4.3 ppm and the vinylic proton peaks of BA, and ii) to estimate the M_n by SEC (THF) (Figure S8). The final CBPQT⁴⁺ end-functionalized poly(*n*-butyl acrylate) **3** was recovered after precipitation in cold hexane. The number-average molar mass was determined by SEC (THF), $M_n = 15600 \text{ g mol}^{-1}$, $D = 1.38$, and by ¹H NMR (CD₃CN), $M_n = 15100 \text{ g mol}^{-1}$ ($M_{n,\text{th}} = 12844 \text{ g mol}^{-1}$).

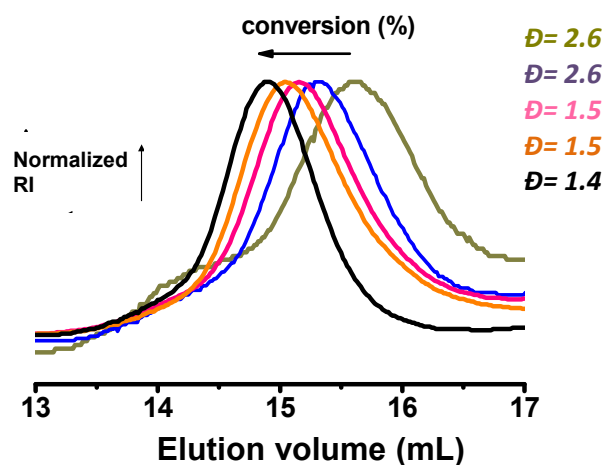


Figure S8. Evolution of the SEC chromatograms for the polymerization of *n*-butyl acrylate in presence of the chain transfer agent **2** initiated by AIBN. Recorded in THF at 40 °C and at a flow rate of 1 mL min⁻¹

¹H NMR (300 MHz, CD₃CN), δ (ppm from TMS) : 8.95-8.77 (brs, 8H), 8.21-8.11 (brs, 8H), 7.64-7.29 (brs, 7H), 5.92-7.76 (brs, 8H), 5.13 (s, 2H), 4.03-3.99 (brs, CH₃(CH₂)₂-CH₂-O), 3.31 (d, *J*= 6.8 Hz, 2H), 2.33-2.16 (brs, CH₂CH backbone), 1.85-1.83 (brs, CH₂CH backbone), 1.67-1.33 (brs, CH₃(CH₂)₂-CH₂-O and CH₂CH backbone), 0.95-0.90 (brs, CH₃-(CH₂)₂-CH₂-O).

IR (cm⁻¹, KBr): 2959, 2959, 2934, 2874, 1730, 1638, 1450, 1395, 1378, 1242, 1158, 1117, 1063, 1022, 961, 941, 839, 785, 738.

Synthesis of naphthalene end-functionalized Poly(*N,N*-dimethylacrylamide) **6b**

A mixture of *N,N*-dimethylacrylamide (2.1 g, 21.0 mmol, 145 eq.), AIBN (2.5 mg, 0.015 mmol, 0.1 eq.) and **CTA-Napht** (84.9 mg, 0.145 mmol, 1 eq.) in DMF (6.2 mL) was deoxygenated by bubbling argon for 30 min in ice water and was then immersed in an oil bath at 70 °C. Samples were periodically withdrawn to measure the conversion by ¹H NMR by comparing the integrated areas of characteristic signals of monomer and polymer. The final polymer was recovered by precipitation of the mixture into diethyl ether. After filtration, the product was dried under vacuum, and the number-average molar mass was determined by SEC (DMF), $M_n = 10120 \text{ g mol}^{-1}$, $D = 1.12$ and by ¹H NMR (acetone-*d*₆), $M_n = 14400 \text{ g mol}^{-1}$ ($M_{n,\text{th}} = 11359 \text{ g mol}^{-1}$).

Synthesis of TTF end-functionalized Poly(*N,N*-dimethylacrylamide) **7b**

A mixture of *N,N*-dimethylacrylamide (5 g, 50.6 mmol, 224 eq.), AIBN (11.8 mg, 0.072 mmol, 0.3 eq.) and **CTA-TTF** (0.106 g, 0.226 mmol, 1 eq.) in DMF (10 mL) was deoxygenated by bubbling argon for 30 min in ice water and was then immersed in an oil bath at 70°C. Samples were periodically withdrawn to measure the conversion by ¹H NMR by comparing the integrated areas of characteristic signals of monomer and polymer. The final polymer was recovered by precipitation of the mixture into diethyl ether. After filtration, the product was dried under vacuum, and the number-average molar mass was determined by SEC (DMF), $M_n = 11300 \text{ g mol}^{-1}$, $D = 1.10$ and by ¹H NMR (acetone-*d*₆), $M_n = 13150 \text{ g mol}^{-1}$ ($M_{n,\text{th}} = 11760 \text{ g mol}^{-1}$).

III. Characterization of polymers **3, 6a,b** and **7a,b**

a) Characterization of CBPQT⁴⁺ end-functionalized poly(*n*-butyl acrylate) **3**

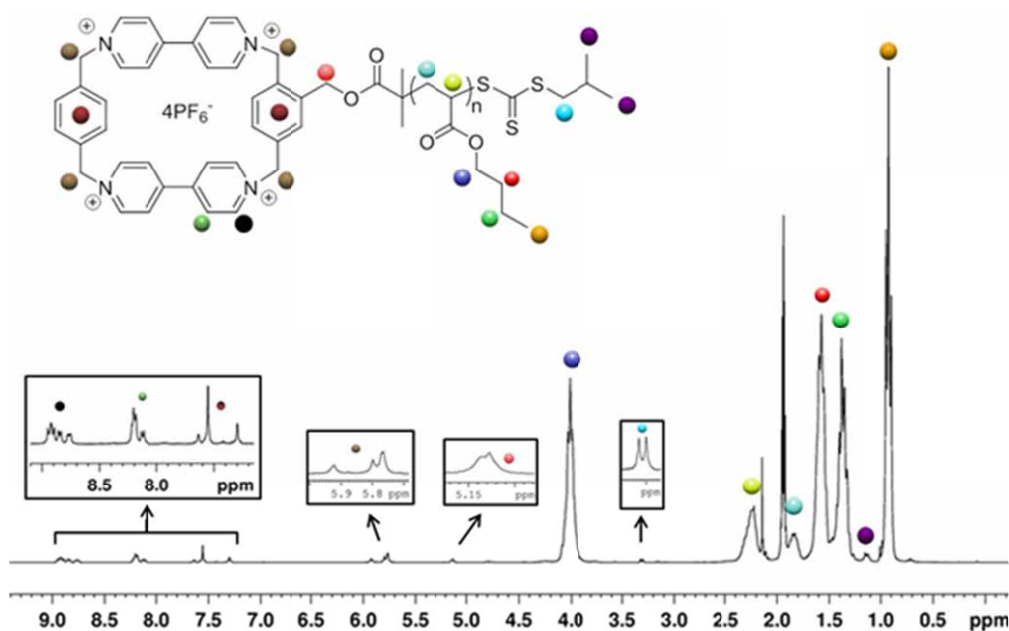


Figure S9. ¹H NMR spectrum of **3** recorded in CD₃CN at 298K

Determination of $M_{n,\text{RMN}}$:

$$M_{n,\text{RMN}} = \frac{I_{\text{pol}}/n_{\text{pol}}}{I_{\text{CTA}}/n_{\text{CTA}}} \times M_{\text{monomer}} + M_{\text{CTA}}$$

$M_{n,\text{RMN}}$: Number-average molar mass, M_n , determined by NMR.

I_{pol} : Integration area of a polymer characteristic signal

n_{pol} : Protons number corresponding to I_{pol} .

I_{CTA} : Integration area of a transfer agent characteristic signal

n_{CTA} : Protons number corresponding to I_{CTA}

M_{monomer} : Monomer molecular weight (g mol⁻¹)

M_{CTA} : Transfer (RAFT) agent molecular weight (g mol⁻¹)

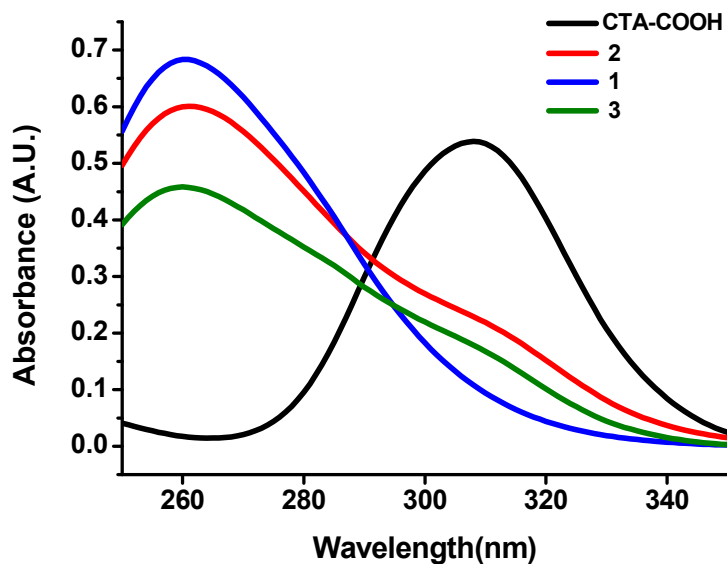


Figure S10. UV-vis spectra of **1** (blue curve), **2** (red curve), **CTA-COOH** (black curve) and **3** (green curve) recorded in CH_3CN (0.5 mM) at 298K.

The UV-vis spectrum of **3** reveals the presence of the trithiocarbonate group located at the terminus of the polymer chain.

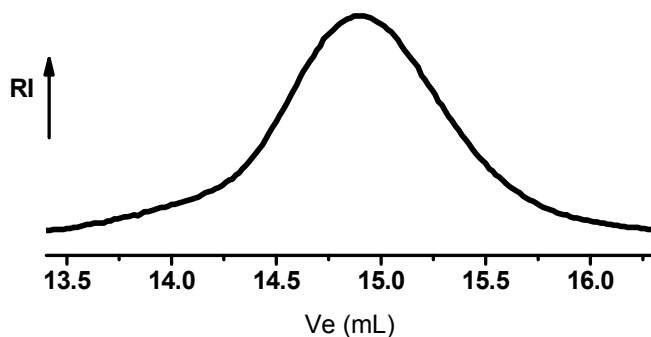


Figure S11. SEC trace of **3**. Recorded in THF at 40 °C and at a flow rate of 1 mL min^{-1}

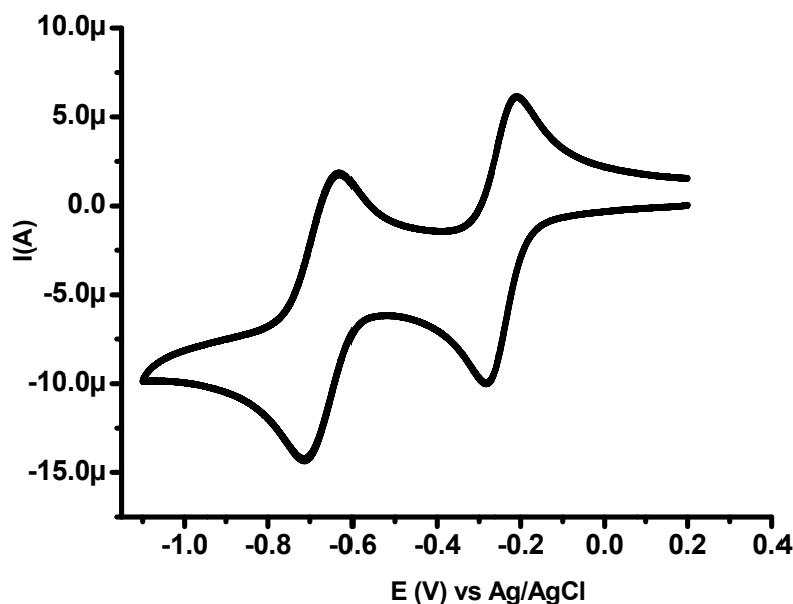


Figure S12. Cyclic voltammogram of **3** (0.5 mM) recorded in acetonitrile in the presence of Bu_4NPF_6 (0.1 M) at a scan rate of 50 mV s⁻¹. Platinum as working electrode and Ag/AgCl as reference electrode

The Polymer **3** gives rise to two reversible two-electron reduction waves at -0.29 V and -0.72 V corresponding to the two step reduction of the CBPQT⁴⁺ unit.³

b) Characterization of naphthalene end-functionalized Poly(*N*-isopropylacrylamide) **6a**

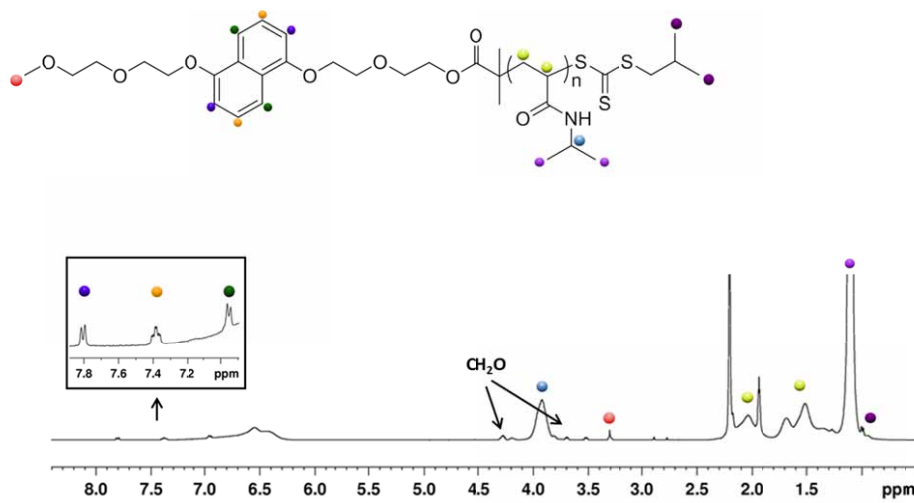


Figure S13. ¹H NMR spectrum of **6a** recorded in CD_3CN at 298 K

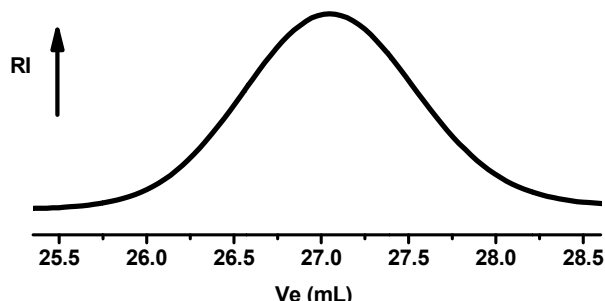


Figure S14. SEC trace of **6a**. Recorded in DMF (+ LiBr, 1 g L⁻¹) at 60 °C and at a flow rate of 0.8 mL min⁻¹

c) Characterization of Naphthalene end-functionalized Poly(*N,N*-dimethylacrylamide) **6b**

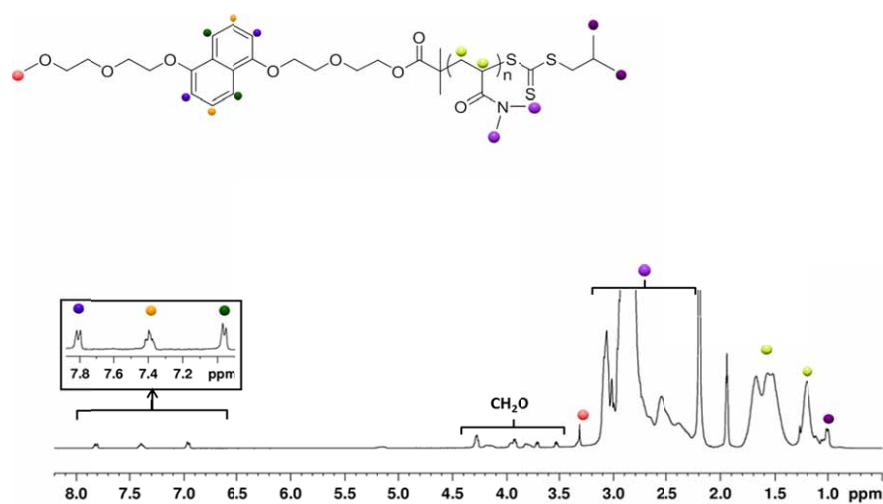


Figure S15. ¹H NMR spectrum of **6b** recorded in CD₃CN at 298 K

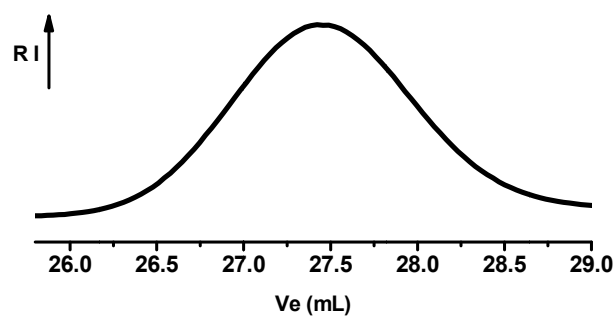


Figure S16. SEC trace of **6b**. Recorded in DMF (+ LiBr, 1 g L⁻¹) at 60 °C and at a flow rate of 0.8 mL min⁻¹

d) Characterization of TTF end-functionalized Poly(*N*-isopropylacrylamide) **7a**

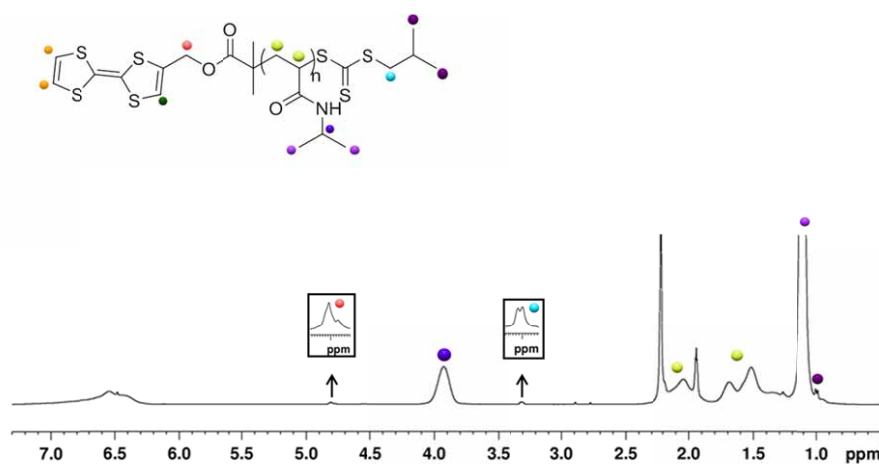


Figure S17. ¹H NMR spectrum of **7a** recorded in CD₃CN at 298 K

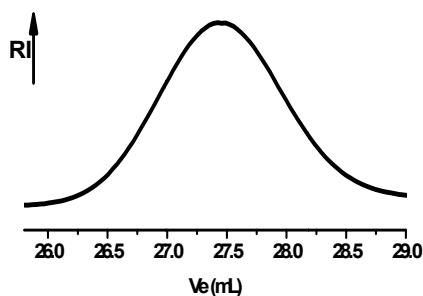


Figure S18. SEC trace of **7a**. Recorded in DMF (+ LiBr, 1 g L⁻¹) at 60 °C and at a flow rate of 0.8 mL min⁻¹

e) Characterization of TTF end-functionalized Poly(*N,N*-dimethylacrylamide) **7b**

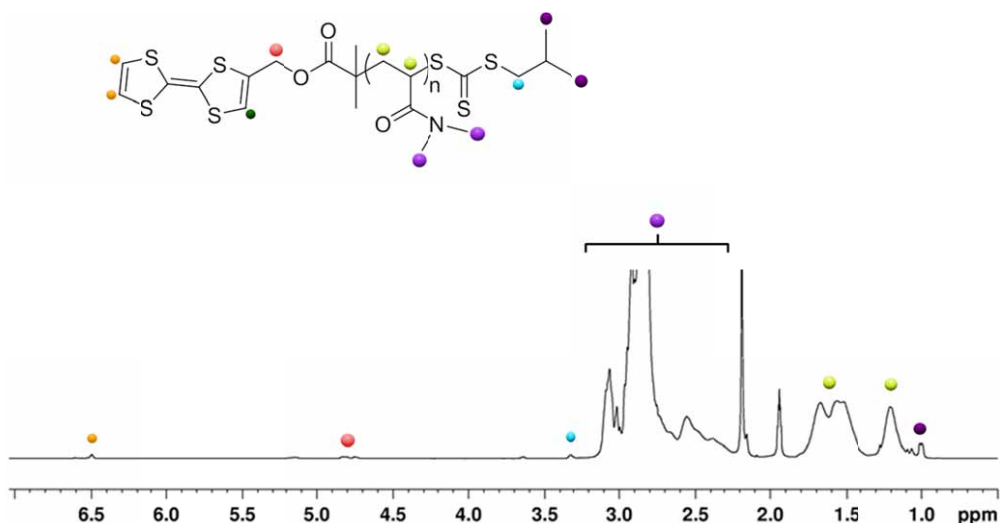


Figure S19. ¹H NMR spectrum of **7b** recorded in CD₃CN at 298 K

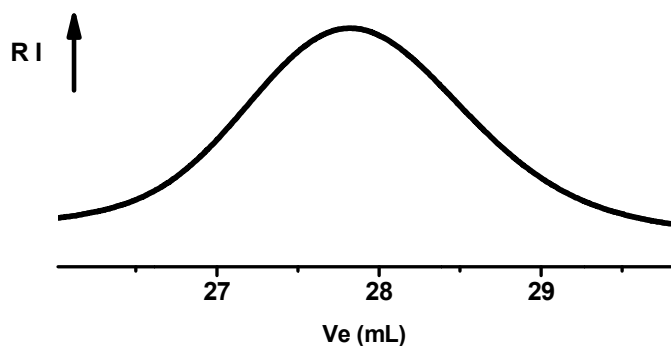


Figure S20. SEC trace of **7b**. Recorded in DMF (+ LiBr, 1 g L⁻¹) at 60 °C and at a flow rate of 0.8 mL min⁻¹

D) Binding studies

I. Binding studies between **3** and **4**

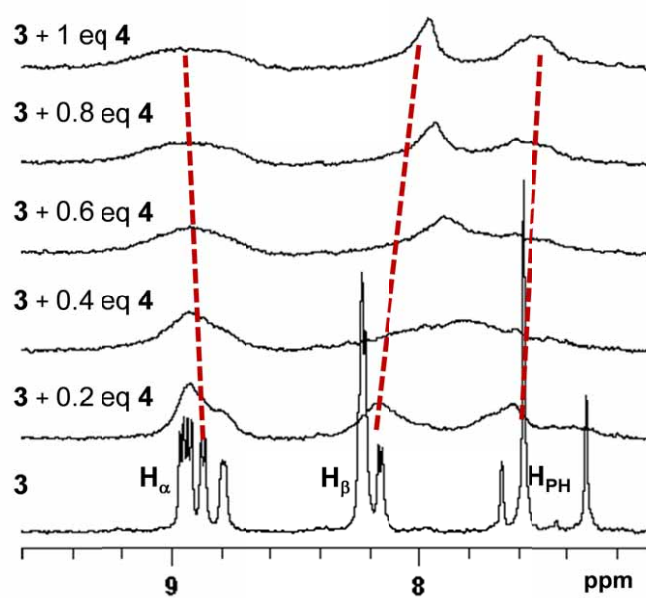


Figure S21 Partial ¹H NMR spectrum of **3** (0.5 mM) in the presence of various equivalents of **4**. Recorded in CD₃CN at 298 K

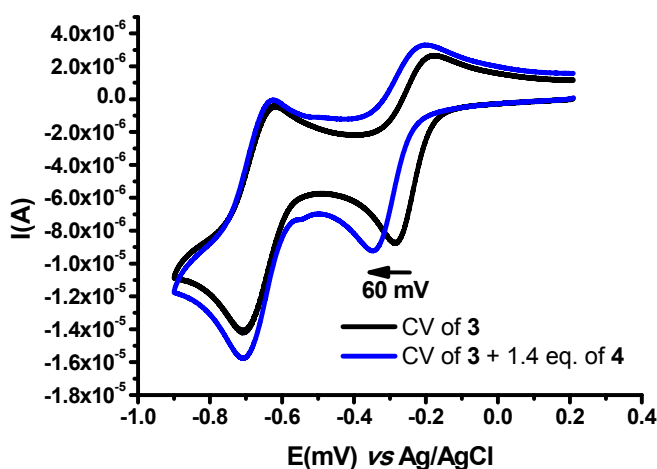


Figure S22. Cyclic voltammogram of **3** (0.5 mM) in the presence of **4** recorded in acetonitrile in the presence of Bu_4NPF_6 (0.1 M) at a scan rate of 50 mV s⁻¹. Platinum as working electrode and Ag/AgCl as reference electrode

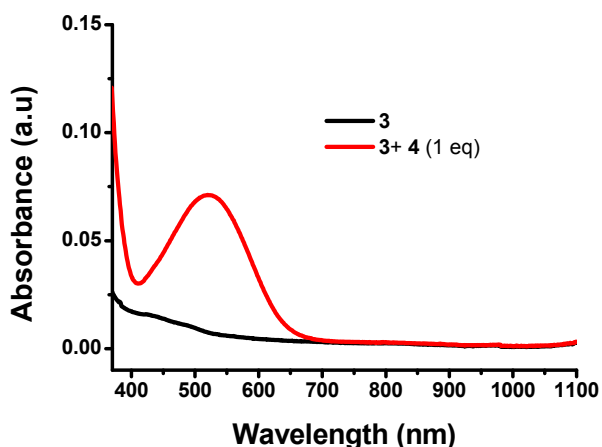


Figure S23. UV-vis spectra of **3** recorded before (dark curve) and after (red curve) the addition of 1 eq. of **4**. Conditions: [3] = 1 mM in CD_3CN , 298 K

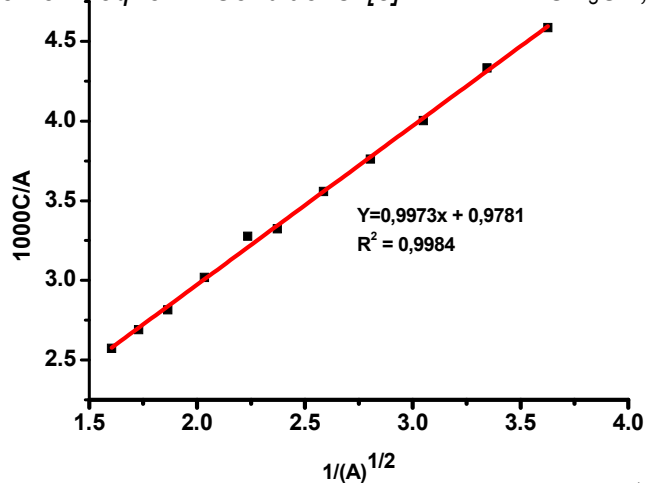


Figure S24. UV-vis dilution experiment: linear plot of C/A against $1/A^{1/2}$ for a 1:1 mixture of **3** and **4**. K_a (3.4) $\approx 9.8 \times 10^2 \text{ M}^{-1}$

II) Binding studies between **3** and **5**

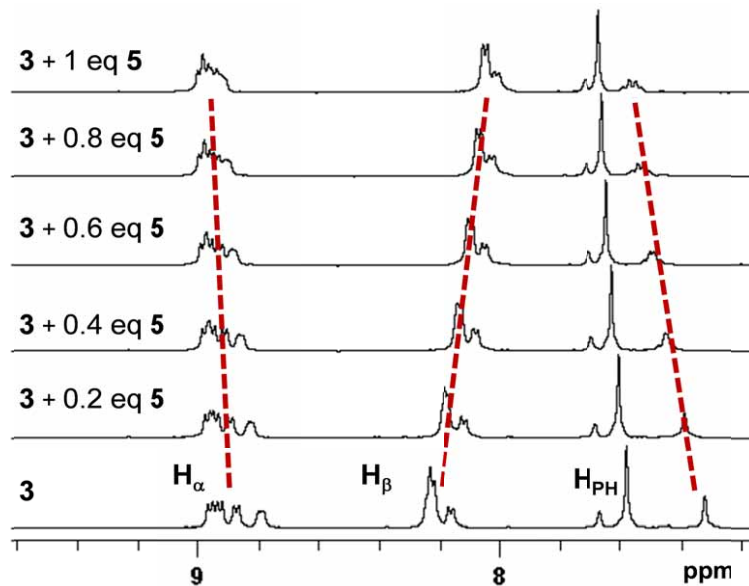


Figure S25. Partial ¹H NMR spectrum of **3** recorded in the presence of various amounts of **5**.
Recorded in CD₃CN at 298 K

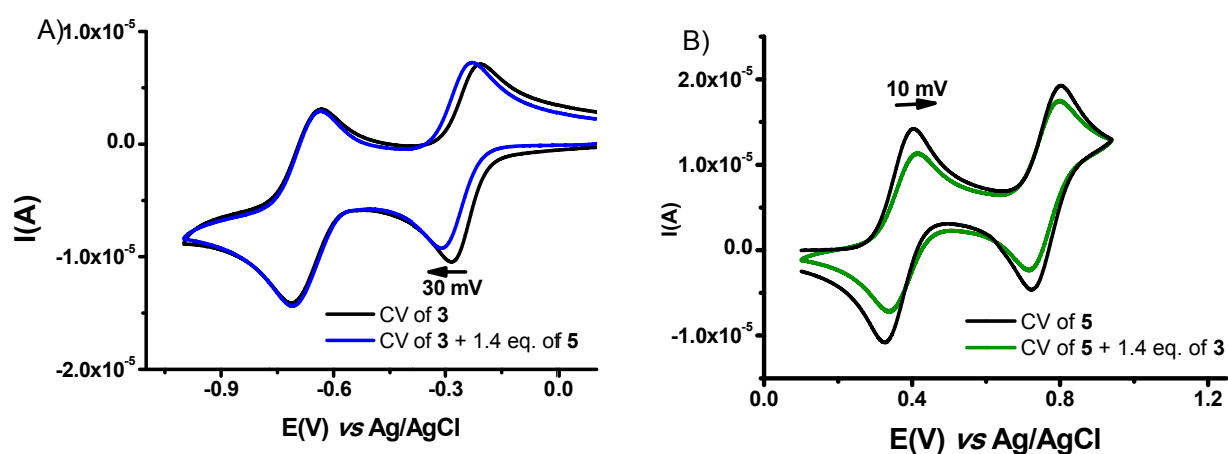


Figure S26. Cyclic voltammograms of (A) **3** (0.5 mM) in the presence of **5** and (B) **5** in the presence of **3**. Recorded in acetonitrile in the presence of Bu₄NPF₆ (0.1 M) at a scan rate of 50 mV s⁻¹. Platinum as working electrode and Ag/AgCl as reference electrode

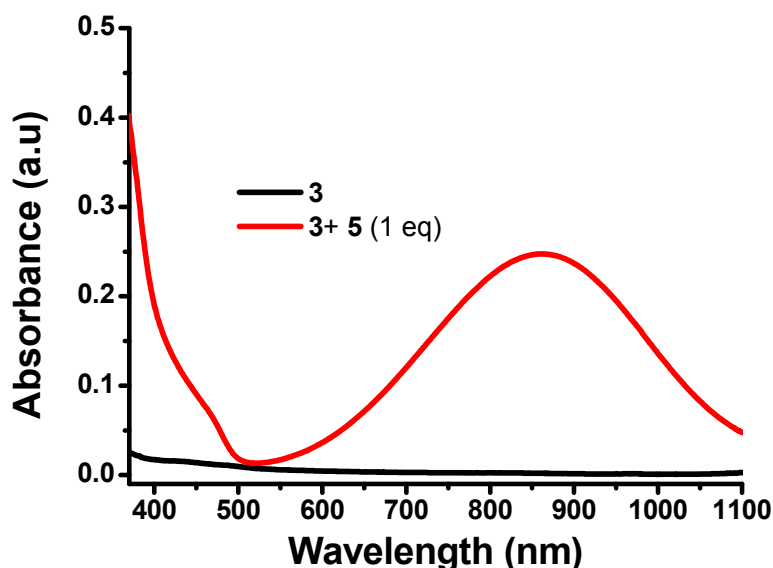


Figure S27. UV-vis spectra of **3** recorded before (dark curve) and after the addition (red curve) of 1 eq. of **5**. Conditions: $[3] = 1\text{ mM}$ in CD_3CN , 298 K.

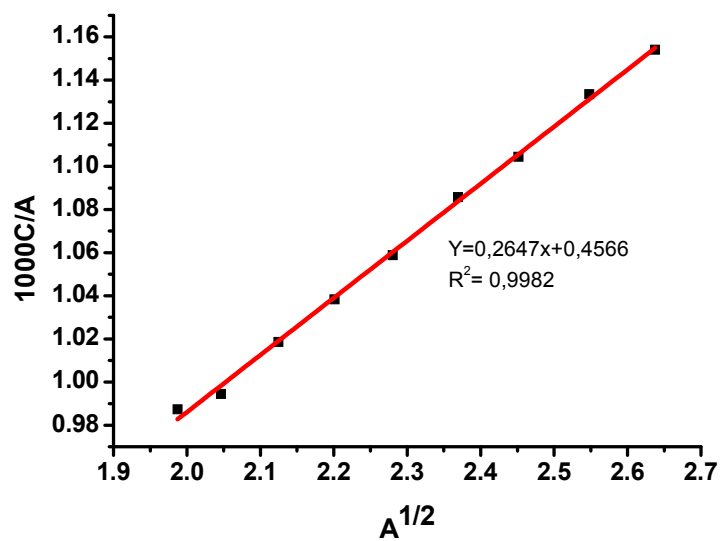


Figure S28. UV-vis dilution experiment: linear plot of C/A against $1/\text{A}^{1/2}$ for a 1:1 mixture of **3** and **5**. K_a (**3.5**) $\approx 6.5 \times 10^3\text{ M}^{-1}$

III) Binding studies between 3 and 6a

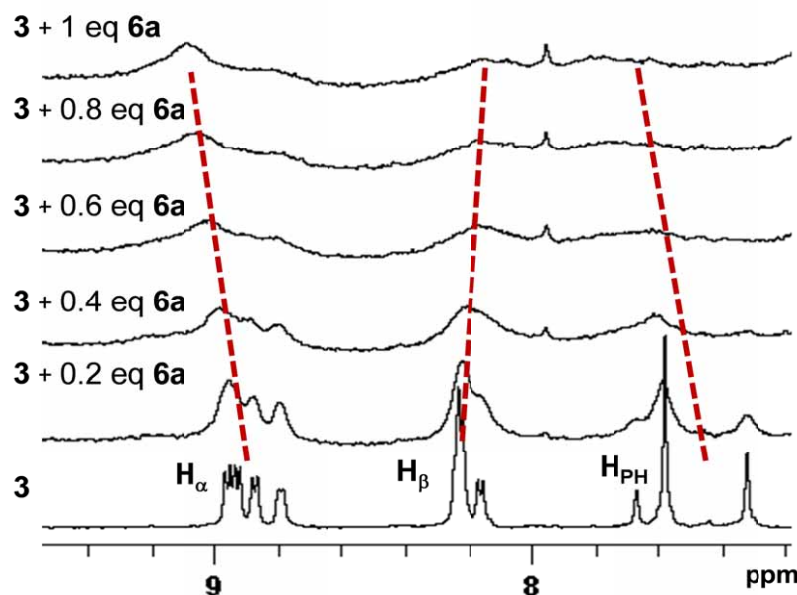


Figure S29. Partial ^1H NMR spectrum of 3 (0.5 mM) recorded in the presence of various amounts of 6a. Recorded in CD_3CN at 298 K

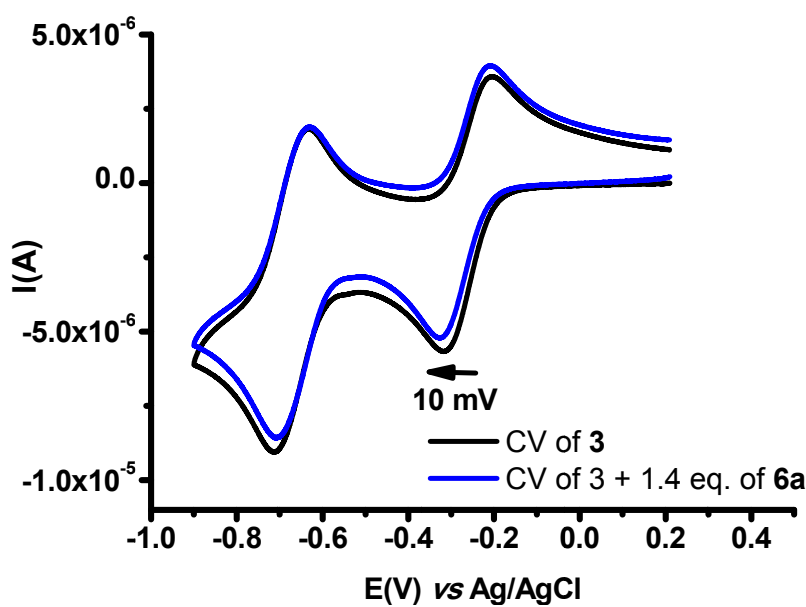


Figure S30. Cyclic voltammograms of 3 (0.5 mM) before (dark curve) and after the addition (blue curve) of 6a recorded in acetonitrile in the presence of Bu_4NPF_6 (0.1 M) at a scan rate of 50 mV s⁻¹. Platinum as working electrode and Ag/AgCl as reference electrode

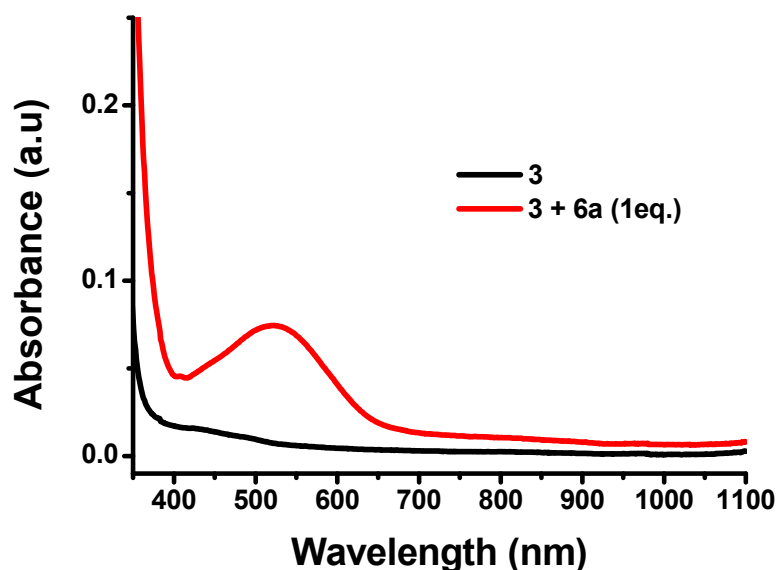


Figure S31. UV-vis spectra of **3** recorded before (dark curve) and after the addition (red curve) addition of 1 eq. of **6a**. Conditions: $[3] = 1\text{ mM}$ in CD_3CN , 298 K

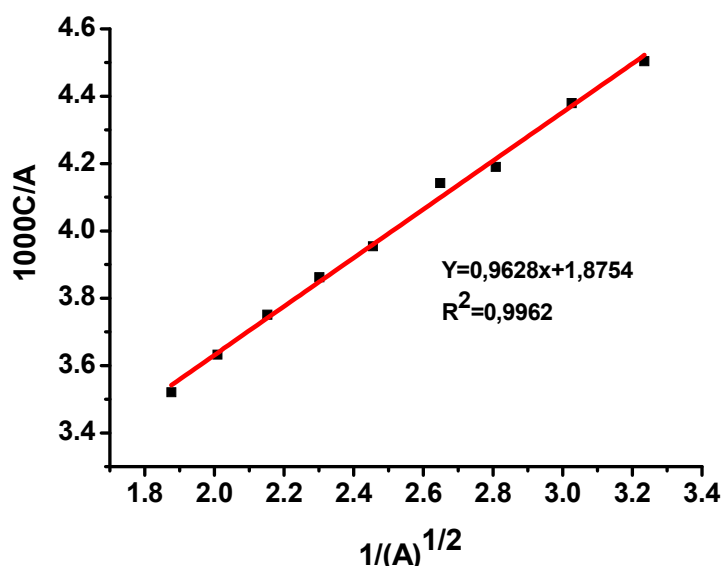


Figure S32. UV-vis dilution experiment: linear plot of C/A against $1/A^{1/2}$ for a 1:1 mixture of **3** and **6a**. $K_a(3.6a) \approx 2.0 \times 10^3 \text{ M}^{-1}$

IV) Binding studies between **3 and **6b****

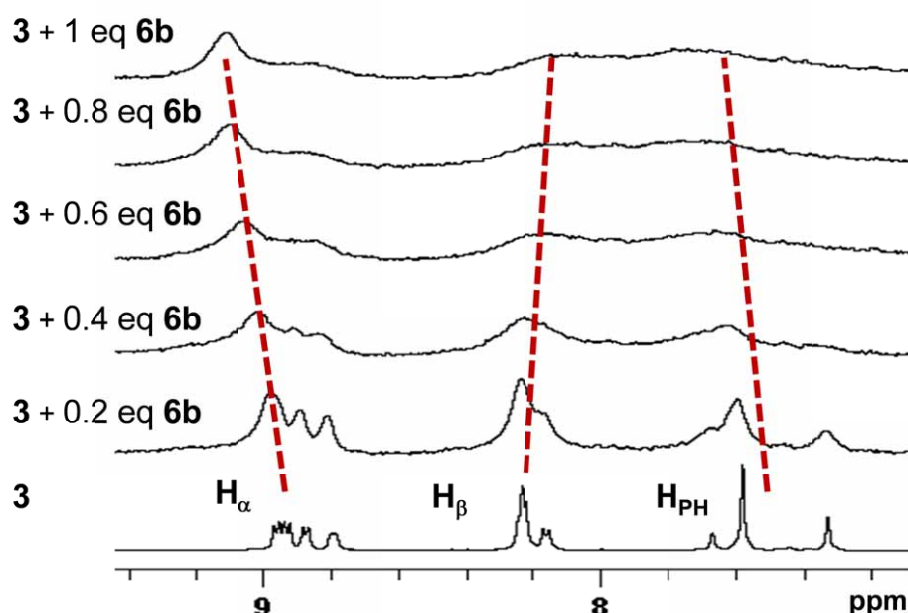


Figure S33 Partial ^1H NMR spectrum of **3** (0.5 mM) recorded in the presence of various amounts of **6b**. Recorded in CD_3CN at 298K

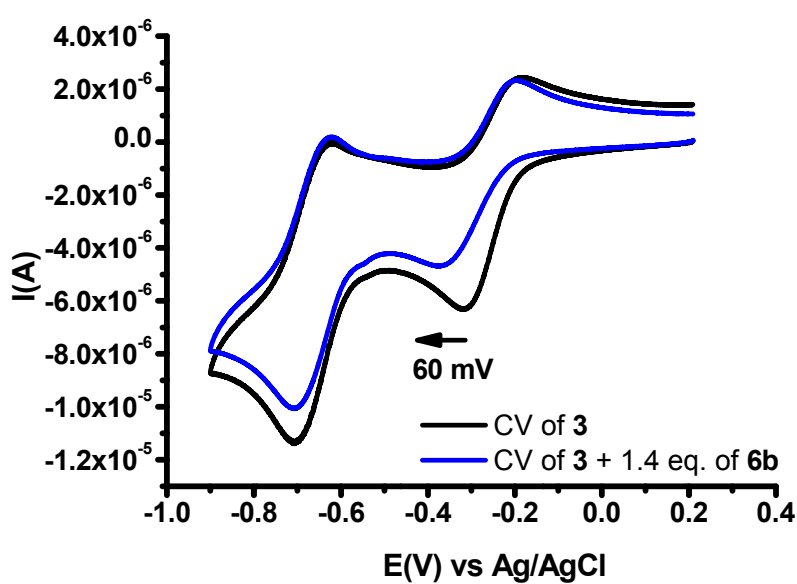


Figure S34. Cyclic voltammograms of **3** (0.5 mM) recorded before (dark curve) and after the addition (blue curve) of **6b** recorded in acetonitrile in the presence of Bu_4NPF_6 (0.1M) at a scan rate of 50 mV/s. Platinum as working electrode and Ag/AgCl as reference electrode

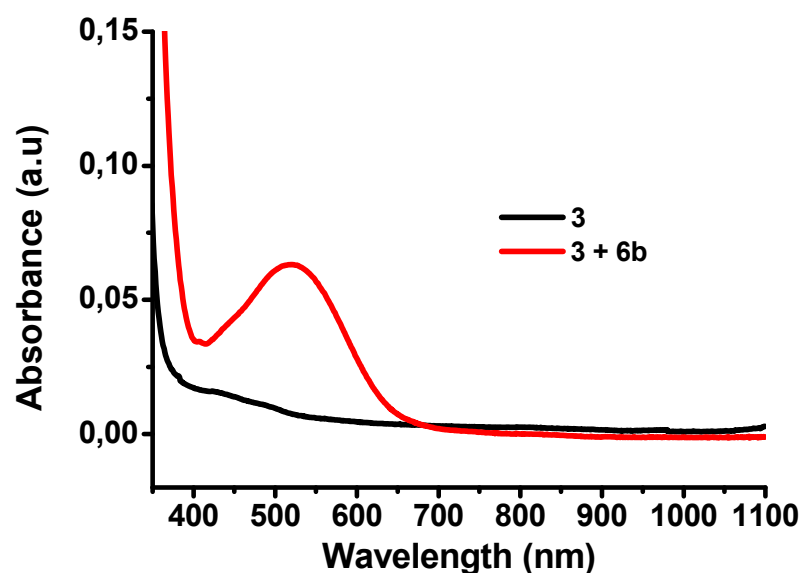


Figure S35. UV-vis spectra of **3** recorded before (dark curve) and after the addition (red curve) of 1 eq. of **6b**. Conditions: $[3] = 1\text{ mM}$ in CD_3CN , 298K

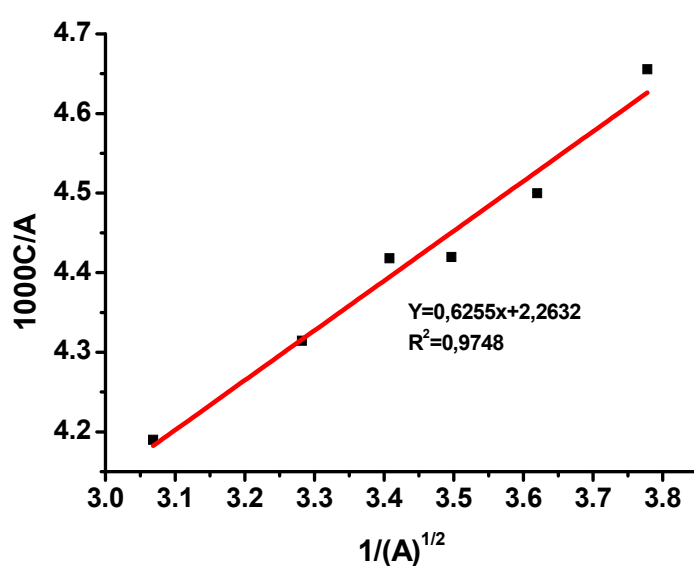


Figure S36. UV-vis dilution experiment :Linear plot of C/A against $1/\text{A}^{1/2}$ for a 1:1 mixture of **3** and **6**. K_a (**3.6b**) $\approx 5.8 \times 10^3\text{ M}^{-1}$

V) Binding studies between **3** and **7a**

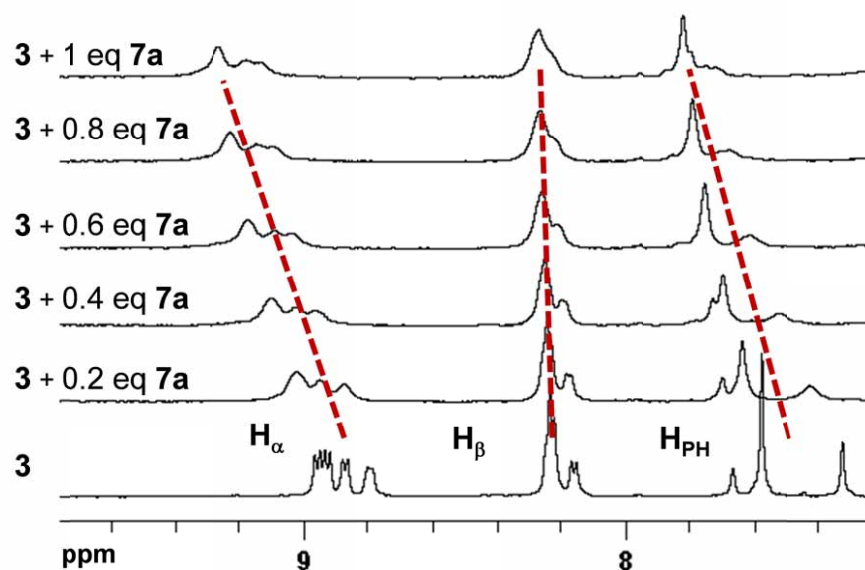


Figure S37. Partial ¹H NMR spectrum of **3** recorded in the presence of various amounts of **7a**

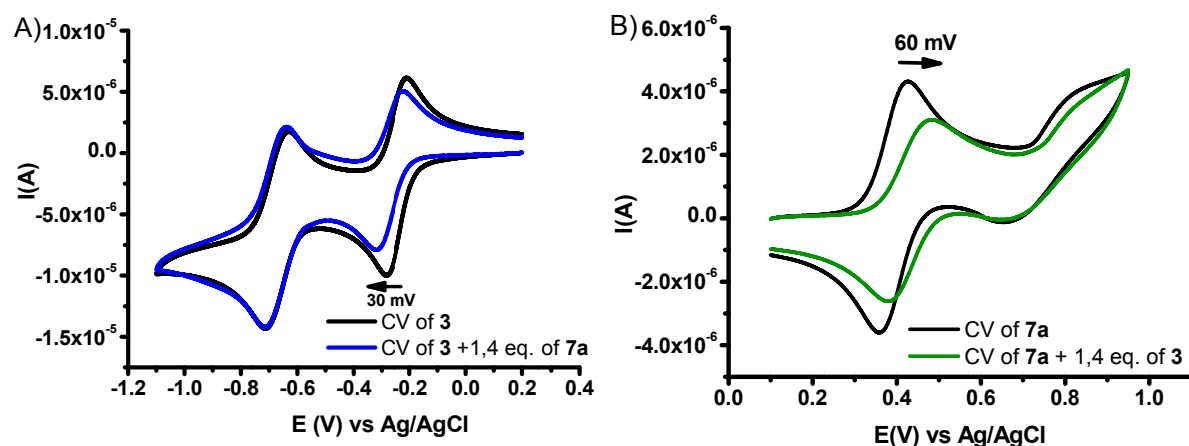


Figure S38. Cyclic voltammograms of (A) **3** (0.5 mM) in the presence of **7a** and (B) **7a** in the presence of **3**. Recorded in acetonitrile in the presence of Bu_4NPF_6 (0.1 M) at a scan rate of 50 mV s⁻¹. Platinum as working electrode and Ag/AgCl as reference electrode

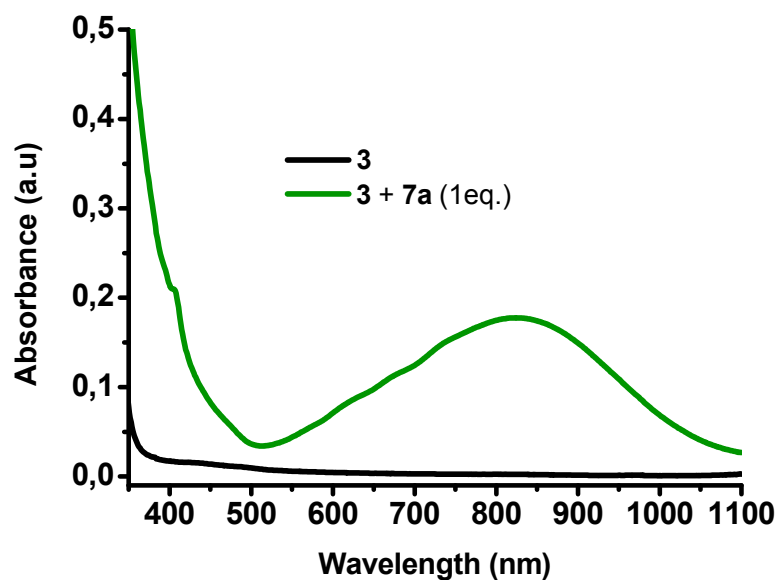


Figure S39. UV-vis spectra of **3** recorded before (dark curve) and after (green curve) the addition of 1 eq. of **7a**. Conditions: $[3] = 1\text{ mM}$ in CD_3CN , 298 K

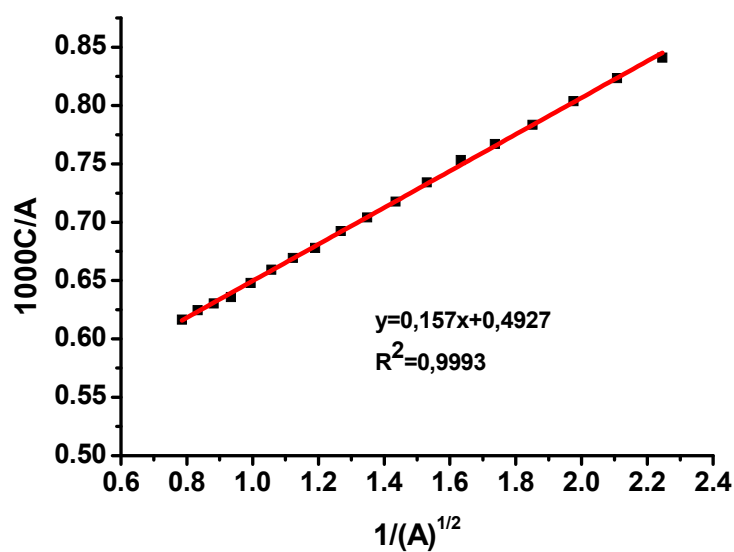


Figure S40. UV-vis dilution experiment: linear plot of C/A against $1/\text{A}^{1/2}$ for a 1:1 mixture of **3** and **7a**. K_a (**3.7a**) $\approx 2.0 \times 10^4 \text{ M}^{-1}$

VI) Binding studies between **3** and **7b**

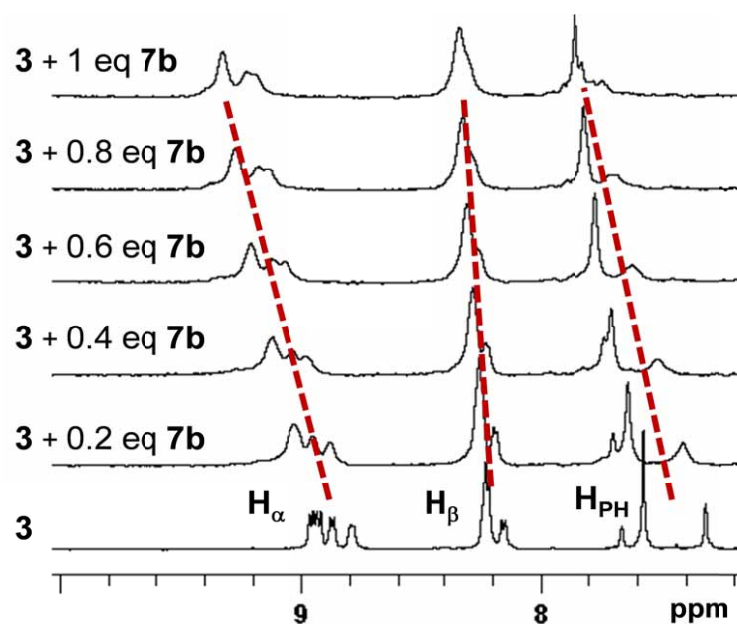


Figure S41. Partial ¹H NMR spectrum of **3** (0.5 mM) recorded in the presence of various amounts of **7b**

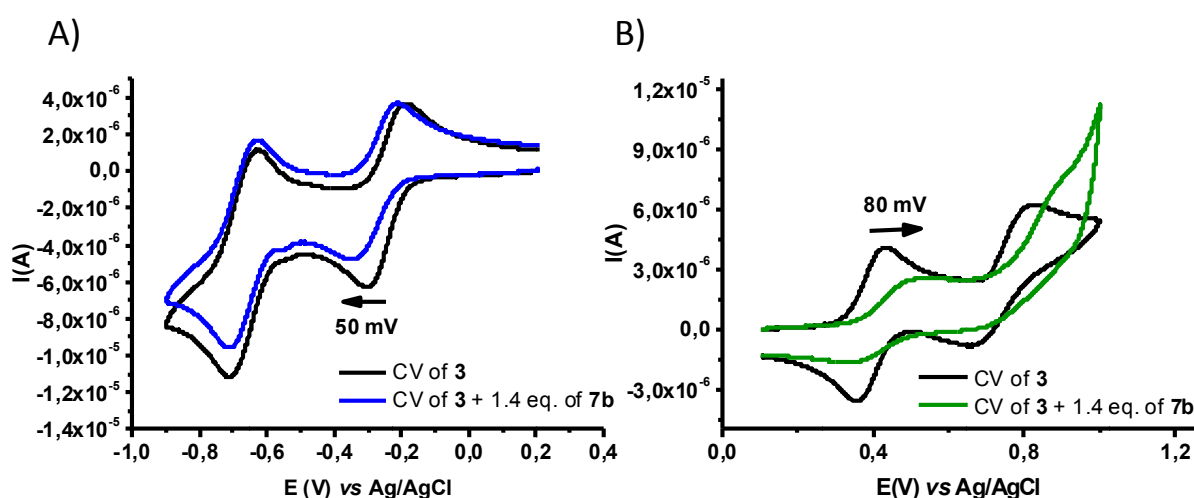


Figure S42. Cyclic voltammetry studies of **3** and **7b** recorded upon the addition of **7b** (Figure A) and **3** (Figure B), respectively. Recorded in acetonitrile in the presence of Bu₄NPF₆ (0.1 M) at a scan rate of 50 mV s⁻¹. Platinum as working electrode and Ag/AgCl as reference electrode.

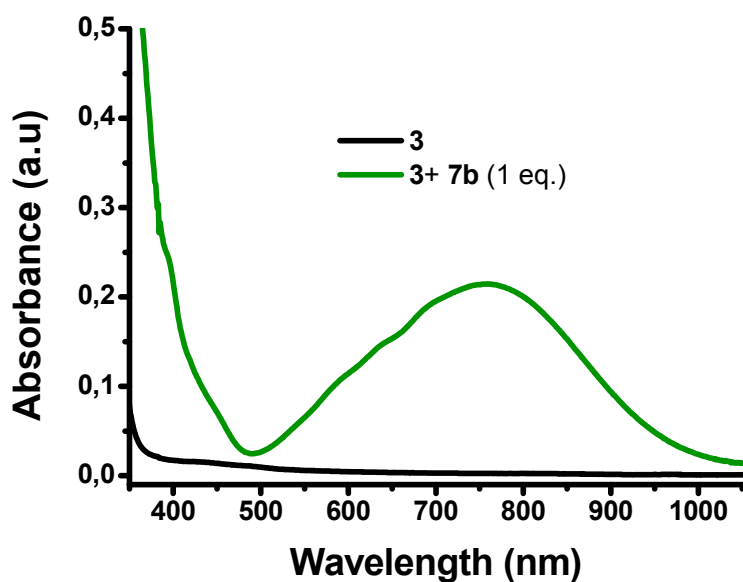


Figure S43. UV-vis spectra of **3** recorded before (dark curve) and after (green curve) the addition of 1 eq. of **7b**. Conditions: $[3] = 1\text{ mM}$ in CD_3CN , 298 K

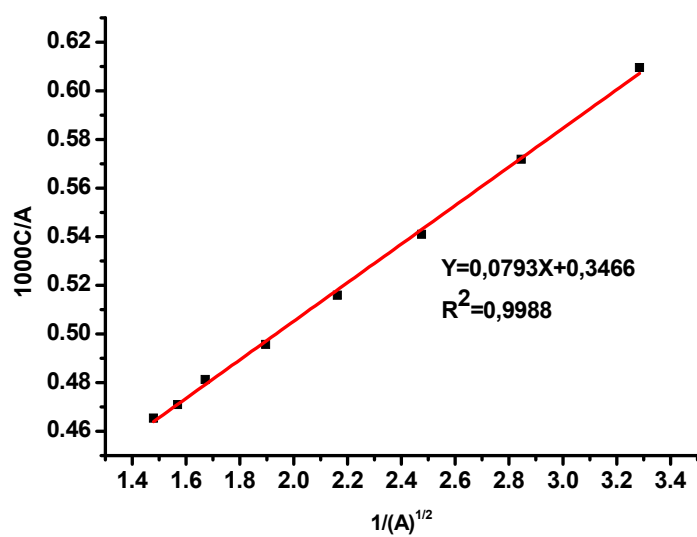


Figure S44. UV-vis dilution experiment: linear plot of C/A against $1/A^{1/2}$ for a 1:1 mixture of **3** and **7b** $K_a(3.7b) \approx 5.5 \times 10^4 \text{ M}^{-1}$

VII) Binding studies: Summary of ^1H NMR and voltammetric data

Table 1. The ^1H NMR chemical shifts (δ and $\Delta\delta$) for **3** and its complexes with **4**, **5**, **6a,b** and **7a,b** in CD_3CN at 298 K.

compounds or complexes	H_α	H_β	H_{Ph}
3	8.92	8.21	7.55
3.4	8.98	7.94	7.51
$\Delta\delta$	(+0.06)	(-0.27)	(-0.05)
3.5	8.96	8.02	7.65
$\Delta\delta$	(+0.04)	(-0.19)	(+0.09)
3.6a	9.05	8.13	7.76
$\Delta\delta$	(+0.14)	(+0.08)	(+0.20)
3.6b	9.09	8.11	7.72
$\Delta\delta$	(+0.18)	(-0.10)	(+0.17)
3.7a	9.24	8.25	7.79
$\Delta\delta$	(+0.32)	(+0.04)	(+0.24)
3.7b	9.30	8.31	7.84
$\Delta\delta$	(+0.38)	(+0.10)	(+0.28)

Table 2. The potential shifts (ΔE) for **3** and its complexes with **4**, **5**, **6a,b**, **7a,b** in CD_3CN at 298K.

Complexes	ΔE Red (mV)	ΔE Ox (mV)
3.4	-60	-
3.6a	-10	-
3.6b	-60	-
3.5	-30	+10
3.7a	-30	+60
3.7b	-50	+80

VIII) Control of binding events upon heating: UV-vis data

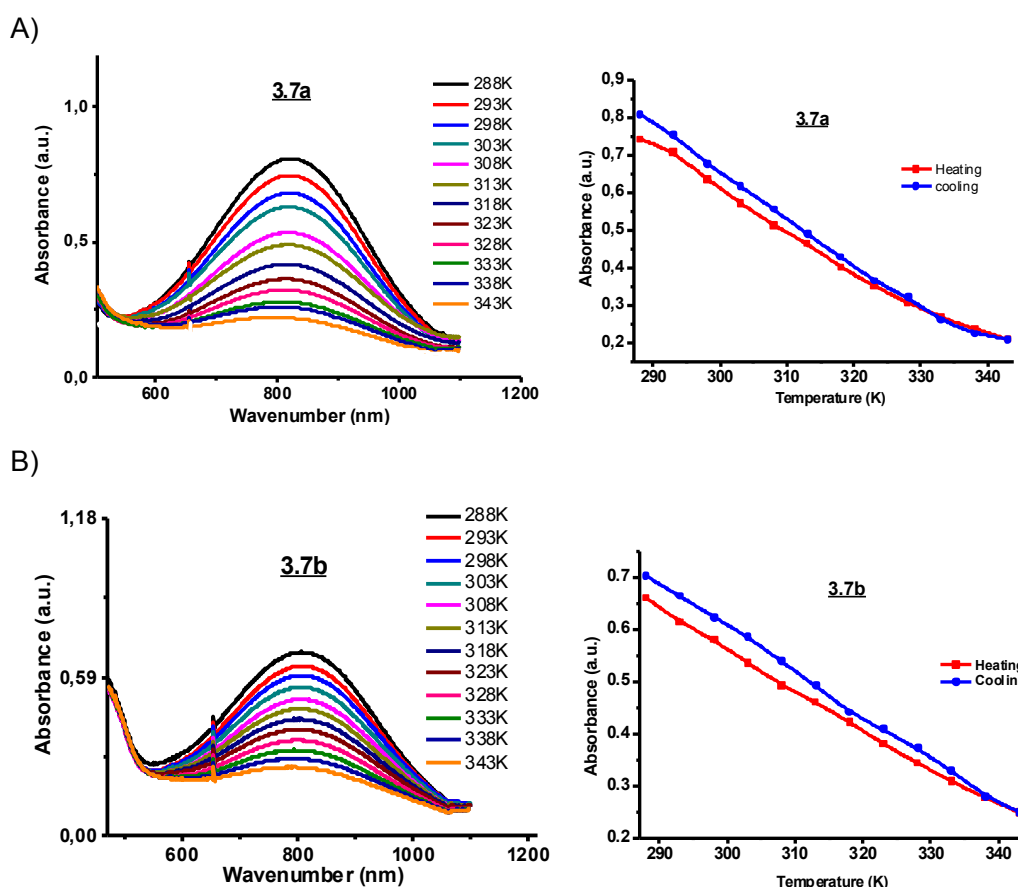


Figure S45 UV-vis spectra of **3.7a** (A) and **3.7b** (B) upon cycling the temperature between 288 K and 343 K. Recorded in acetonitrile at 0.5 mM

IX) Control of binding events upon the addition of TTF: UV-vis and ^1H NMR data

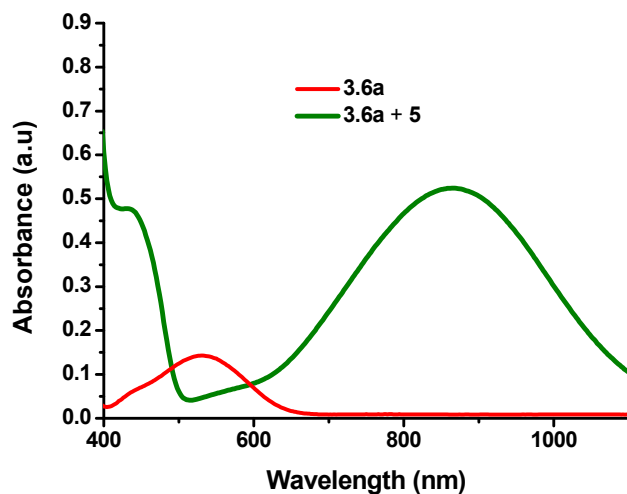


Figure S46 UV-vis spectra of **3.6a** (red curve) and **3.6a** upon the addition of **5** (1.4 equiv.) (green curve). Recorded in acetonitrile at 298 K at 0.5 mM

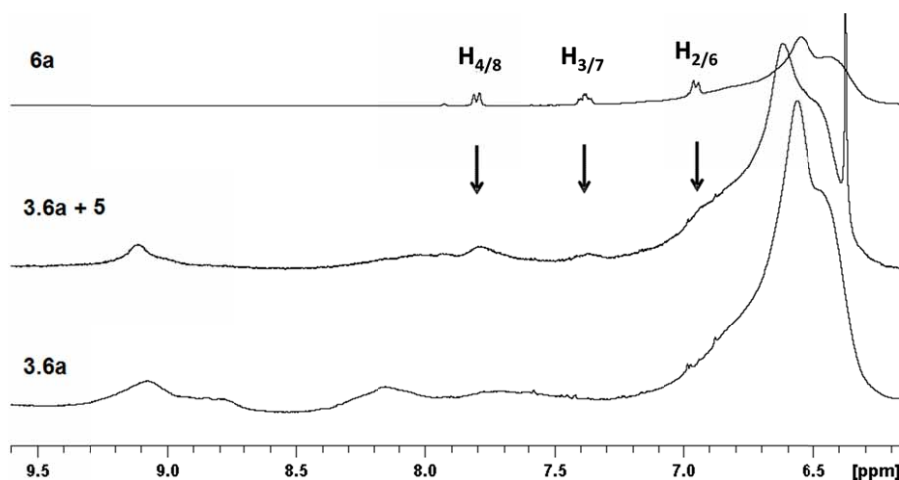


Figure S47. Partial ¹H NMR spectra of **6a**, **3.6a** and **3.6a** upon the addition of **5** (1 equiv.).
Recorded in CD₃CN at 298 K at 0.5 mM

E) Nanostructuration of **3.7b** in water and in thin films: UV-vis and AFM data

Atomic Force Microscopy (AFM)

AFM images were recorded using a commercial AFM (NanoScope VIII MultiMode AFM, Bruker Nano Inc., Nano Surfaces Division, Santa Barbara, CA) equipped with a 150 × 150 × 5 μm scanner (J-scanner). The substrates were fixed on a steel sample puck using a small piece of adhesive tape. Images were recorded in peak force tapping mode in air at room temperature (22–24 °C) using oxide-sharpened microfabricated Si₃N₄ cantilevers (Bruker Nano Inc., Nano Surfaces Division, Santa Barbara, CA). The spring constants of the cantilevers were measured using the thermal noise method, yielding values ranging from 0.4 to 0.5 N m⁻¹. The curvature radius of silicon nitride tips was about 10 nm (manufacturer specifications). All images shown in this paper are flattened data using a third-order polynomial.

Cryo-transmission electron microscopy (cryo-TEM)

Cryo-TEM was used to determine the morphology and size of the polymer nanoparticles. According to protocols reported elsewhere^{8, 9} thin liquid films of particle dispersions, prepared at room temperature, were flash frozen in liquid ethane and observed at -180 °C on a JEOL JEM-2100 LaB₆ microscope (Cs = 2.0 mm) operating at 200 kV under low-dose conditions (10 electrons Å⁻² s⁻¹). Digital images were recorded on a Gatan Ultrascan 1000 CCD camera.

Dynamic light scattering (DLS).

The particle size (hydrodynamic average diameter: $\langle D_h \rangle$) and the dispersity (Poly) of aqueous dispersions of **7b** and **3.7b** (both at 0.52 mM) were measured by DLS (NanoZS from Malvern Instruments) at 90° at 25 °C.

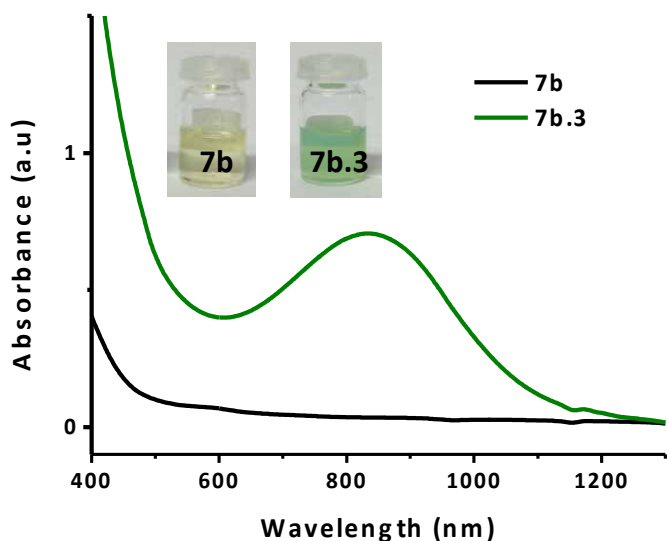


Figure S48. UV-vis spectra of **7b** (dark curve) and **3.7b** (green curve), Recorded in water at 298 K at ~ 0.5 mM

Films preparation of block copolymer

Glass substrate was 10*10 mm² microscope coverslip and was washed by immersion in THF and ethanol just before use. The films were obtained either by spin-coating or drop-casting of 5 wt.% block copolymer in THF onto the clean glass substrate. Spin coating was performed as follows: 100 µL of the block copolymer solution were deposited on the substrate and immediately accelerated to 3000 rpm for 50 s. Samples were allowed to dry at room temperature for a minimum of 12 h prior to analysis. Drop-casting was performed as follows: 100 µL of 5 wt.% block copolymer solution in THF were deposited on the substrate followed by slow evaporation at room temperature

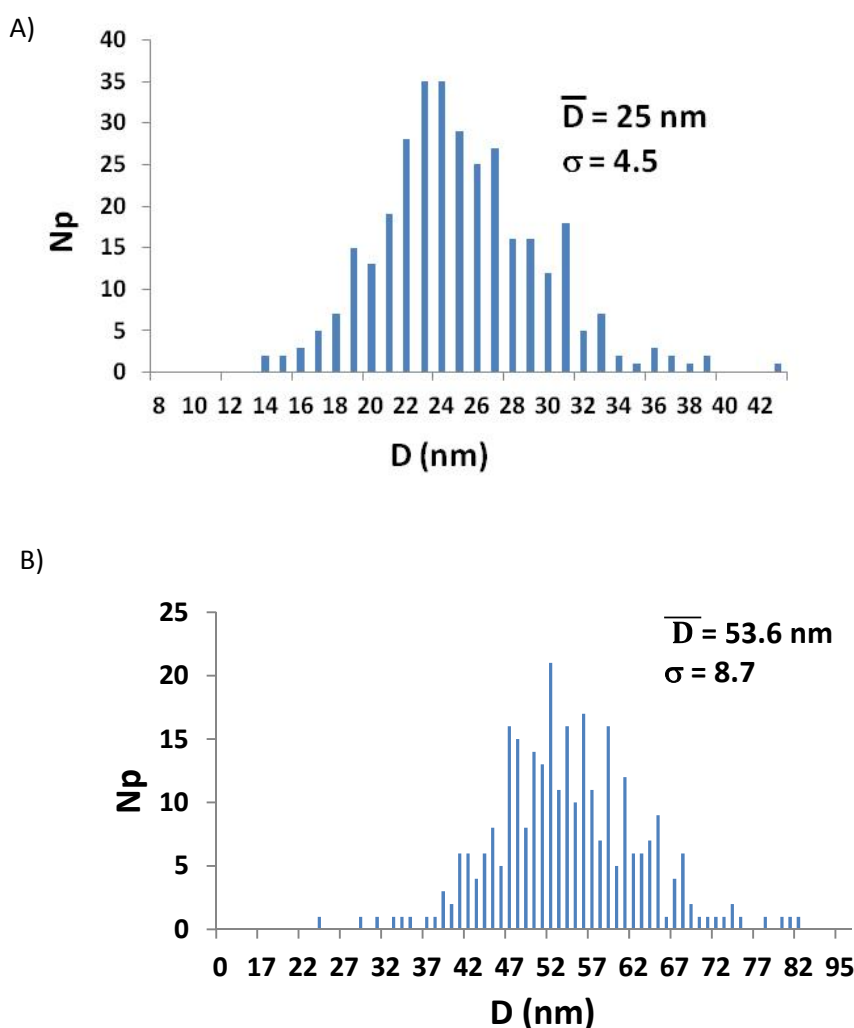


Figure S49. Histograms showing size distribution of micelles based on Cryo-Tem (A) and AFM (B) images.

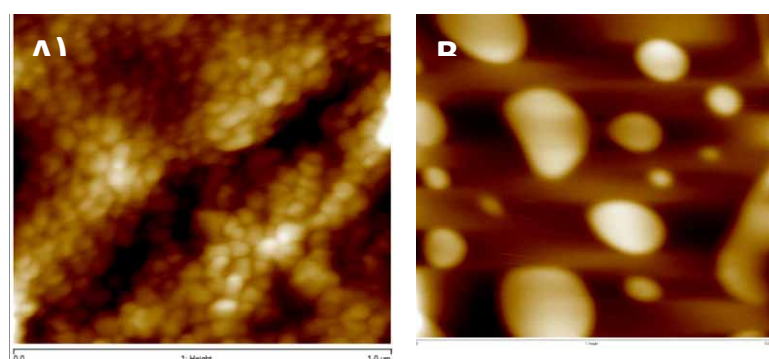


Figure S50. AFM topographic images of a notch in **3.7b** thin films self-assembled on glass substrates prepared by spin coating from a THF solution of **3.7b** at 5 wt% (A). AFM height image of a blend of unfunctionalized poly(*n*-butyl acrylate) with **7b** (C) from a THF solution at 5 wt% (B)

F) References

1. M. B. Nielsen, J. O. Jeppesen, J. Lau, C. Lomholt, D. Damgaard, J. P. Jacobsen, J. Becher and J. F. Stoddart, *J. Org. Chem.*, 2001, **66**, 3559-3563.
2. G. Cooke, J. F. Garety, S. G. Hewage, B. J. Jordan, G. Rabani, V. M. Rotello and P. Woisel, *Org. Lett.*, 2007, **9**, 481-484.
3. P. L. Anelli, P. R. Ashton, R. Ballardini, V. Balzani, M. Delgado, M. T. Gandolfi, T. T. Goodnow, A. E. Kaifer and D. Philp, *J. Am. Chem. Soc.*, 1992, **114**, 193-218.
4. M. J. Gunter, D. C. R. Hockless, M. R. Johnston, B. W. Skelton and A. H. White, *J. Am. Chem. Soc.*, 1994, **116**, 4810-4823.
5. X.-P. Qiu, F. Tanaka and F. M. Winnik, *Macromolecules*, 2007, **40**, 7069-7071.
6. J. Bigot, D. Fournier, J. Lyskawa, T. Marmin, F. Cazaux, G. Cooke and P. Woisel, *Polym. Chem.*, 2010, **1**, 1024-1029.
7. J. Bigot, B. Charleux, G. Cooke, F. Delattre, D. Fournier, J. Lyskawa, F. Stoffelbach and P. Woisel, *Macromolecules*, 2010, **43**, 82-90.
8. M. Adrian, J. Dubochet, J. Lepault and A. W. McDowall, *Nature*, 1984, **308**, 32-36.
9. J. Dubochet, M. Adrian, J. J. Chang, J.-C. Homo, J. Lepault, A. W. McDowall and P. Schultz, *Quart. Rev. Phys.*, 1988, **21**, 129-228.